



NUMERICAL SOLUTION OF THE MULTIGROUP NEUTRON DIFFUSION EQUATION BY THE MESHLESS RBF COLLOCATION METHOD

Tayfun Tanbay and Bilge Ozgener

Institute of Energy, Istanbul Technical University, 34469, Maslak, Istanbul, Turkey
ozgenb@itu.edu.tr

Abstract- The multigroup neutron diffusion criticality problem is studied by the radial basis function collocation method. The multiquadric is chosen as the radial basis function. To investigate the effectiveness of the method, one, two and three-group problems are considered. It is found that the radial basis function collocation method produces highly accurate multiplication factors and it is also efficient in the calculation of group fluxes.

Key Words- Neutron diffusion, Radial basis function collocation, Multiquadric

1. INTRODUCTION

Numerical solution of the neutron diffusion equation has been done by many numerical methods such as the finite difference, finite element and boundary element methods. These are all mesh-based methods in which the nodes that discretize the problem domain are related in a predefined manner. In this paper we apply a novel, meshless technique, the radial basis function (RBF) collocation method, for the numerical solution of the neutron diffusion equation.

Meshless methods have emerged in late 70's and became an alternative class of numerical tools for the solution of differential and integral equations. As their name implies, the nodes do not have to satisfy any relation. The analyst can distribute them uniformly or randomly. There are many meshless methods in literature with different mathematical properties. For details, we refer the readers to Liu [1].

The RBF collocation method was proposed by Kansa [2] and has found itself a wide application area [3-5] over the past decades. It is a strong-form meshless method and unlike the weak-form meshless methods it is a truly meshless one since there is no integration in the solution procedure. There is numerical evidence that the method has an exponential convergence rate [6] and it is shown to be more accurate than the finite difference, finite element with linear shape functions and spectral methods [7,8]. On the other hand the method is less stable than weak-form meshless or mesh-based methods, but the high level of accuracies that can be obtained by fewer nodes motivates the use of this approximation scheme.

2. FORMULATION OF THE PROBLEM

This study deals with the numerical solution of the multigroup neutron diffusion criticality problem and for a square homogeneous system with reflective boundary conditions at its bottom and left sides and with vacuum boundary conditions at its right and top sides the problem can be mathematically written as

$$-D_g \nabla^2 \varphi_g^{(n)} + \Sigma_{r,g} \varphi_g^{(n)} = \sum_{g'=1}^{g-1} \Sigma_{s,g' \rightarrow g} \varphi_{g'}^{(n)} + \frac{1}{\lambda^{(n-1)}} \chi_g F^{(n-1)}, 0 \leq x \leq a, 0 \leq y \leq a \quad (1)$$

$$\begin{aligned} \frac{\partial \varphi_g}{\partial y}(x, 0) &= 0, 0 \leq x \leq a \\ \varphi_g(a, y) &= 0, 0 \leq y \leq a \\ \varphi_g(x, a) &= 0, 0 \leq x \leq a \\ \frac{\partial \varphi_g}{\partial x}(0, y) &= 0, 0 \leq y \leq a \end{aligned} \quad (2)$$

where $g = 1, \dots, G$. Here g and n denote the energy group and the iteration index, respectively, G is the total number of energy groups, D is the diffusion constant, φ is the neutron flux, λ is the multiplication factor, χ is the fission spectrum function, ν is the number of neutrons per fission, Σ_r, Σ_s and Σ_f are macroscopic removal, scattering and fission cross sections, respectively and a is the size of the domain. F is the fission source and it is defined as

$$F \equiv \sum_{g'=1}^G \nu_{g'} \Sigma_{f,g'} \varphi_{g'} \quad (3)$$

The system of equations, Eq. (1), is solved by fission source iteration, which starts by guessing the fission source and the multiplication factor as $F \sim F^{(0)}, \lambda \sim \lambda^{(0)}$. Next, the neutron flux of the first group, $\varphi_1^{(1)}$, is calculated. Then, by using this flux, $\varphi_2^{(1)}$ and neutron fluxes of the following groups can be found. After that a new fission source and a multiplication factor is determined by

$$F^{(1)} = \sum_{g'=1}^G \nu_{g'} \Sigma_{f,g'} \varphi_{g'}^{(1)} \quad \lambda^{(1)} = \lambda^{(0)} \frac{\int d\Omega F^{(1)}}{\int d\Omega F^{(0)}} \quad (4)$$

where $d\Omega$ is the area element. This iterative strategy goes on until a predetermined convergence criterion is satisfied

$$\left| \frac{\lambda^{(n+1)} - \lambda^{(n)}}{\lambda^{(n+1)}} \right| < \epsilon \quad (5)$$

For the formulation we first introduce a set of internal nodes with N_I members such that:

$$I = \{(x_i, y_i) : 0 < x_i < a, 0 < y_i < a, 1 \leq i \leq N_I\} \quad (6)$$

Then we introduce a set of reflective boundary nodes with $N_B/2$ members such that:

$$B_R = B_{RB} \cup B_{RL} \quad (7)$$

where B_{RB} represent a set of reflective boundary nodes on the bottom side while B_{RL} represent a set of reflective boundary nodes on the left side. That is:

$$\begin{aligned}
 B_{RB} &= \left\{ (x_i, 0) : 0 \leq x_i < a, N_I < i \leq N_I + \frac{N_B}{4} \right\} \\
 B_{RL} &= \left\{ (0, y_i) : 0 < y_i \leq a, N_I + \frac{3N_B}{4} < i \leq N_I + N_B \right\}
 \end{aligned} \tag{8}$$

Also a set of vacuum boundary nodes B_V with $N_B/2$ members are introduced such that

$$B_V = B_{VR} \cup B_{VT} \tag{9}$$

where B_{VR} represent a set of vacuum boundary nodes on the right side while B_{VT} represent a set of vacuum boundary nodes on the top side. That is

$$\begin{aligned}
 B_{VR} &= \left\{ (0, y_i) : 0 \leq y_i < a, N_I + \frac{N_B}{4} < i \leq N_I + \frac{N_B}{2} \right\} \\
 B_{VT} &= \left\{ (x_i, 0) : 0 < x_i \leq a, N_I + \frac{N_B}{2} < i \leq N_I + \frac{3N_B}{4} \right\}
 \end{aligned} \tag{10}$$

Then, the set of boundary nodes B simply

$$B = B_R \cup B_V = (B_{RB} \cup B_{RL}) \cup (B_{VR} \cup B_{VT}) \tag{11}$$

The set of domain nodes, D is defined as

$$D = I \cup B \tag{12}$$

which represents a set with $N_D = N_I + N_B$ members. Secondly, we introduce a set of external nodes, E . For the purpose of preserving the nonsingularity of the coefficient matrix, the number of members of E has to be equal to N_B . That is

$$E = \{ (x_i, y_i) : [(x_i < 0) \vee (x_i > a)] \wedge [(y_i < 0) \vee (y_i > a)], N_D < i \leq N_D + N_B \} \tag{13}$$

The neutron flux is to be approximated by

$$\varphi_g(x, y) \approx \sum_{j=1}^{N_D+N_B} a_{j,g} \psi_j(x, y) \tag{14}$$

where $\psi_j(x, y)$ is the RBF. For the first part of the collocation process, the neutron diffusion equation is required to hold for (x_i, y_i) such that $1 \leq i \leq N_D$. Then

$$\sum_{j=1}^{N_D} k_{ij,g}^{DD} a_{j,g}^{D,(n)} + \sum_{j=1}^{N_B} k_{ij,g}^{DE} a_{j,g}^{E,(n)} - \sum_{j=1}^{N_D} s_{ij,g' \rightarrow g}^{DD} a_{j,g}^{D,(n)} - \sum_{j=1}^{N_B} s_{ij,g' \rightarrow g}^{DE} a_{j,g}^{E,(n)} = \frac{\chi_g F^{(n-1)}}{\lambda^{(n-1)}} \tag{15}$$

where

$$k_{ij,g}^{DD} = -D_g \left[\frac{\partial^2 \psi_j}{\partial x^2}(x_i, y_i) + \frac{\partial^2 \psi_j}{\partial y^2}(x_i, y_i) \right] + \Sigma_{r,g} \psi_j(x_i, y_i), 1 \leq i \leq N_D, 1 \leq j \leq N_D$$

$$k_{ij,g}^{DE} = -D_g \left[\frac{\partial^2 \psi_{j+N_D}}{\partial x^2}(x_i, y_i) + \frac{\partial^2 \psi_{j+N_D}}{\partial y^2}(x_i, y_i) \right] + \Sigma_{r,g} \psi_{j+N_D}(x_i, y_i), 1 \leq i \leq N_D, 1 \leq j \leq N_B$$

$$s_{ij,g' \rightarrow g}^{DD} = \Sigma_{s,g' \rightarrow g} \psi_j(x_i, y_i), 1 \leq i \leq N_D, 1 \leq j \leq N_D$$

$$s_{ij,g' \rightarrow g}^{DE} = \Sigma_{s,g' \rightarrow g} \psi_{j+N_D}(x_i, y_i), 1 \leq i \leq N_D, 1 \leq j \leq N_B$$

$$a_{j,g}^{D,(n)} = a_{j,g}^{(n)}, 1 \leq j \leq N_D$$

$$a_{j,g}^{E,(n)} = a_{j+N_D,g}^{(n)}, 1 \leq j \leq N_B$$

The collocation is completed by requiring the reflective and vacuum boundary conditions to hold for points (x_i, y_i) which are members of B_R and B_V , respectively.

That is

$$\sum_{j=1}^{N_D} k_{ij}^{BD} a_{j,g}^{D,(n)} + \sum_{j=1}^{N_B} k_{ij}^{BE} a_{j,g}^{E,(n)} = 0, 1 \leq i \leq N_B \quad (16)$$

where

$$k_{ij}^{BD} = \begin{cases} \frac{\partial \psi_j}{\partial y}(x_{i+N_I}, y_{i+N_I}), 1 \leq i \leq \frac{N_B}{4} \\ \frac{\partial \psi_j}{\partial x}(x_{i+N_I}, y_{i+N_I}), \frac{3N_B}{4} < i \leq N_B \\ \psi_j(x_{i+N_I}, y_{i+N_I}), \frac{N_B}{4} < i \leq \frac{3N_B}{4} \end{cases}$$

for $1 \leq j \leq N_D$ and

$$k_{ij}^{BE} = \begin{cases} \frac{\partial \psi_{j+N_D}}{\partial y}(x_{i+N_I}, y_{i+N_I}), 1 \leq i \leq \frac{N_B}{4} \\ \frac{\partial \psi_{j+N_D}}{\partial x}(x_{i+N_I}, y_{i+N_I}), \frac{3N_B}{4} < i \leq N_B \\ \psi_{j+N_D}(x_{i+N_I}, y_{i+N_I}), \frac{N_B}{4} < i \leq \frac{3N_B}{4} \end{cases}$$

for $1 \leq j \leq N_B$.

If there is no upscattering of neutrons then, the two equation sets, Eqs. (15) and (16) result in

$$\begin{bmatrix} \mathbf{K}_1 & \mathbf{0} & \mathbf{0} & \mathbf{0} \\ -\mathbf{S}_{1 \rightarrow 2} & \mathbf{K}_2 & \mathbf{0} & \mathbf{0} \\ \vdots & \vdots & \ddots & \mathbf{0} \\ -\mathbf{S}_{1 \rightarrow G} & -\mathbf{S}_{2 \rightarrow G} & \cdots & \mathbf{K}_G \end{bmatrix} \begin{bmatrix} \mathbf{a}_1^{(n)} \\ \mathbf{a}_2^{(n)} \\ \vdots \\ \mathbf{a}_G^{(n)} \end{bmatrix} = \frac{1}{\lambda^{(n-1)}} \begin{bmatrix} \chi_1 \mathbf{F}^{(n-1)} \\ \chi_2 \mathbf{F}^{(n-1)} \\ \vdots \\ \chi_G \mathbf{F}^{(n-1)} \end{bmatrix} \quad (17)$$

In Eq. (17), the elements of the global system matrix are block matrices themselves. For every energy group an $(N_D + N_B) \times (N_D + N_B)$ system of equations have to be solved. As an example for the first group one has to solve

$$\begin{bmatrix} \mathbf{K}_1^{DD} & \mathbf{K}_1^{DE} \\ \mathbf{K}_1^{BD} & \mathbf{K}_1^{BE} \end{bmatrix} \begin{bmatrix} \mathbf{a}_1^{D,(n)} \\ \mathbf{a}_1^{E,(n)} \end{bmatrix} = \frac{\chi_1}{\lambda^{(n-1)}} \begin{bmatrix} \mathbf{F}_1^{D,(n-1)} \\ \mathbf{0} \end{bmatrix} \quad (18)$$

Here \mathbf{K}_1^{DD} and \mathbf{K}_1^{BE} are square matrices of dimension N_D and N_B respectively. The matrix \mathbf{K}_1^{BD} is rectangular with dimensions $N_B \times N_D$, while \mathbf{K}_1^{DE} is again rectangular with dimensions $N_D \times N_B$. $\mathbf{a}_1^{D,(n)}$ and $\mathbf{F}_1^{D,(n-1)}$ vectors are N_D dimensional while the vector $\mathbf{a}_1^{E,(n)}$ is N_B dimensional. Solution of Eq. (19) yields $\mathbf{a}_1^{D,(n)}$ and hence the numerical result.

There are many RBFs encountered in the literature with different properties. In this study we will employ the multiquadric, which was proposed by Hardy [9] to approximate geographical surfaces

$$\psi_j(x, y) = \sqrt{(x - x_j)^2 + (y - y_j)^2 + c^2} \tag{19}$$

Here, c is called the shape parameter. It determines the shape of the RBF and has an important role in numerical applications. Theoretically, as $c \rightarrow \infty$ the approximation error goes to zero [10]; but this property would be achieved if infinite precision computation could be performed.

3. NUMERICAL RESULTS

To investigate the performance of the RBF collocation method we considered one, two and three group criticality eigenvalue problems. The analytical solutions of these problems can be found in [11]. A program is written in FORTRAN and calculations are performed with double precision. In all tests uniformly scattered nodes are used. The power is assumed to be 16 kW and the convergence criterion is chosen as 10^{-6} for all problems. Accuracy of the method is examined via calculating the error in λ and maximum errors in group fluxes

$$\epsilon_\lambda = |\lambda_a - \lambda_n| \times 100/\lambda_a \tag{20}$$

$$\epsilon_{max,g} = \max_{1 \leq i \leq N_D} [|\phi_{g,a}(x_i) - \phi_{g,n}(x_i)| \times 100/\phi_{g,a}(x_i)] \tag{21}$$

where subscripts a and n denote analytical and numerical, respectively. RBF collocation method is invariant under uniform scaling, hence computations are made on a domain scaled to $[0,1]^2$ by defining the variables $\tilde{x} = x/a$ and $\tilde{y} = y/a$.

In the first problem we studied the one-group case. The length of the square domain is taken as $a = 50 \text{ cm}$, while $D = 1.77764 \text{ cm}$, $\Sigma_f = 0.0104869 \text{ cm}^{-1}$, $\nu = 2.5$, $\Sigma_r = 0.0143676 \text{ cm}^{-1}$ and $\chi = 1$. The analytical value of λ is 1.46657782. Fig.1 shows the variation of ϵ_{max} and ϵ_λ with respect to the reciprocal of the fill distance (distance between adjacent nodes), where $c^2 = 0.06$. It is observed from this figure that ϵ_{max} decreases continuously with decreasing value of the fill distance. It has its minimum value of 5.642×10^{-3} when $h^{-1} = 36$. Highly accurate λ values are obtained above $h^{-1} = 22$ and, the percent error has decreased to its minimum of 4.091×10^{-6} when $h^{-1} = 32$.

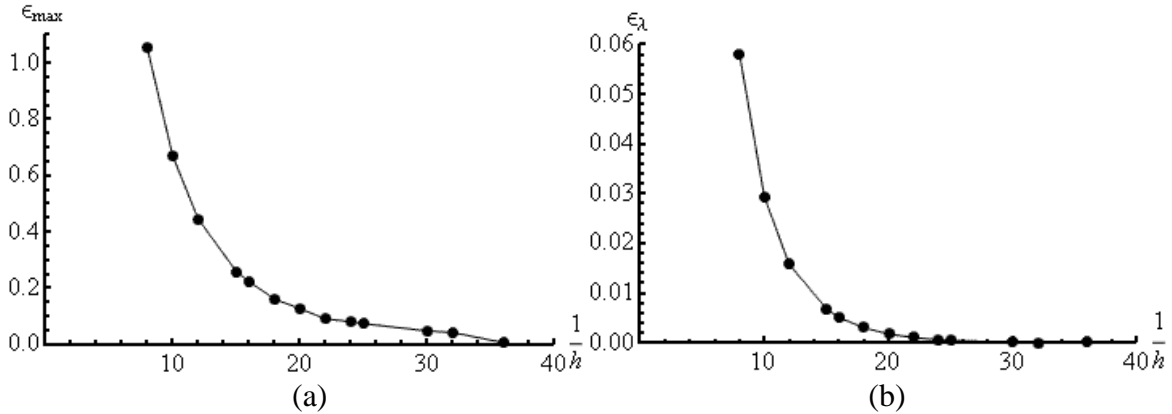


Figure 1. Variation of (a) ϵ_{max} and (b) ϵ_λ with respect to the fill distance

In the second problem the number of energy groups is two and $a = 25 \text{ cm}$. The nuclear data is given in Table 1. Diffusion constants are given in units of centimeters and all cross sections have units of inverse centimeters in Table 1 and later on in Table 3. For this problem $\lambda_a = 1.96293774$.

Table 1. Two-group nuclear data

Group	D	ν	Σ_f	Σ_r	$\Sigma_{s,g \rightarrow g+1}$	χ
1	1.2245	2.65	0.063	0.13552	0.0676	0.575
2	1.2245	2.55	0.06776	0.08228	-	0.425

The numerical results of the two-group problem are summarized in Table 2 where $c^2 = 0.06$. We see that the maximum errors in group fluxes are similar and decrease with decreasing fill distance value. For the multiplication factor, a very high level of accuracy is obtained above $h^{-1} = 16$. It is also observed from this table that the number of iterations increases by one when $h^{-1} = 32$.

Table 2. ϵ_{max} and ϵ_λ for the two-group problem

$1/h$	n_{iter}	$\epsilon_{max,1}$	$\epsilon_{max,2}$	ϵ_λ
8	29	1.040	1.060	3.221×10^{-2}
12	29	4.429×10^{-1}	4.478×10^{-1}	8.663×10^{-3}
16	29	2.222×10^{-1}	2.236×10^{-1}	2.691×10^{-3}
20	29	1.274×10^{-1}	1.277×10^{-1}	8.238×10^{-4}
24	29	8.173×10^{-2}	8.161×10^{-2}	1.722×10^{-4}
28	29	5.550×10^{-2}	5.502×10^{-2}	7.132×10^{-5}
32	30	4.361×10^{-2}	4.298×10^{-2}	9.730×10^{-5}
36	30	8.136×10^{-3}	7.384×10^{-3}	1.365×10^{-4}

In Fig. 2 the variation of $\epsilon_{max,1}$ and $\epsilon_{max,2}$ with the shape parameter of the multiquadric is illustrated where a fill distance of $h = 0.04 \text{ cm}$ is chosen. The maximum pointwise errors in flux for both groups decrease continuously with increasing shape parameter up to $c^2 \cong 0.12$. Beyond this value the errors start to oscillate and the numerical solution breaks down except for $c^2 = 0.149$. This is

expected since as the shape parameter increases the collocation matrix becomes more and more ill-conditioned.

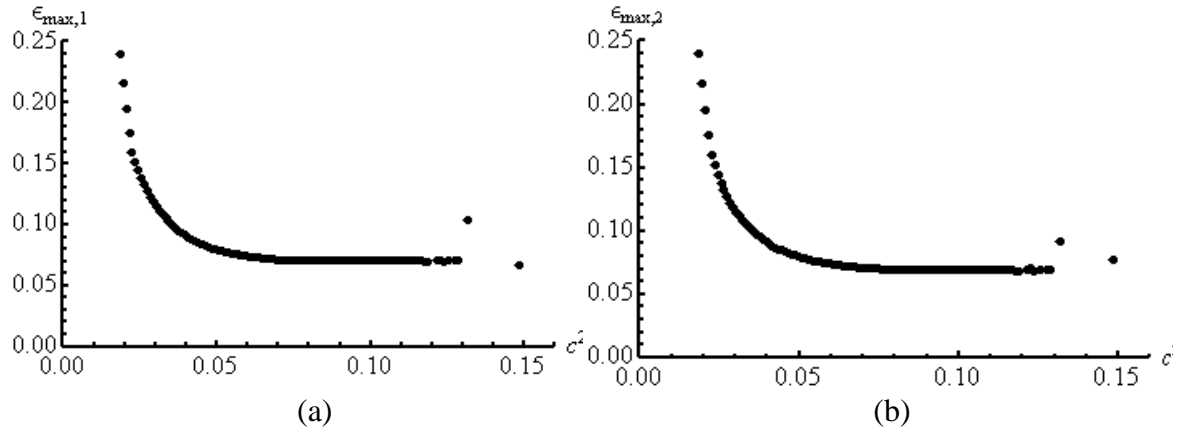


Figure 2. Variation of (a) $\epsilon_{max,1}$, (b) $\epsilon_{max,2}$ with respect to the shape parameter

The error in multiplication factor is shown in Fig. 3 where, again $h = 0.04 \text{ cm}$. It is seen that the error increases with the shape parameter at first up to $c^2 = 0.015$ and then starts to decrease until $c^2 = 0.072$ where the analytical solution is reproduced. Above this value it increases again, and similar to the pointwise errors in group fluxes the numerical solution oscillates and breaks down above $c^2 \cong 0.12$.

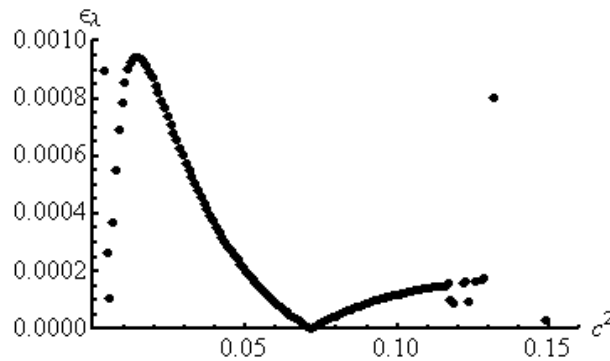


Figure 3. Variation of ϵ_λ with respect to the shape parameter

It should be noted that the change of errors in flux and multiplication factor with the shape parameter is found to be similar for the one and three-group problems also.

The third problem deals with the solution of the three-group neutron diffusion equation where a is assumed to be 25 cm . The nuclear data characterizing a three-group structure is given in Table 3 and the analytical value of λ is 0.75024241 for this problem.

Table 3. Three-group nuclear data

Group	D	ν	Σ_f	Σ_r	$\Sigma_{s,g \rightarrow g+1}$	$\Sigma_{s,g \rightarrow g+2}$	χ
1	3.0034	2.65	0.0131267	0.05286	0.02705	0.01181	0.575
2	2.2297	2.53	0.006102	0.016704	0.00822	-	0.326
3	1.4627	2.47	0.008317	0.01414	-	-	0.099

The number of iterations, maximum pointwise errors for the three group fluxes and the error in λ is given in Table 4 for different fill distance values where $c^2 = 0.06$. Once again, it is found that the errors in group fluxes and multiplication factor decrease with decreasing value of the fill distance. Highly accurate λ values are obtained when the fill distance is 0.05 cm or less. It is also observed that the number of iterations does not depend on the choice of h .

Table 4. ϵ_{max} and ϵ_k for the three-group problem

$1/h$	n_{iter}	$\epsilon_{max,1}$	$\epsilon_{max,2}$	$\epsilon_{max,3}$	ϵ_λ
8	12	9.715×10^{-1}	1.068	1.116	1.702×10^{-1}
12	12	4.232×10^{-1}	4.494×10^{-1}	4.624×10^{-1}	4.649×10^{-2}
16	12	2.149×10^{-1}	2.234×10^{-1}	2.276×10^{-1}	1.519×10^{-2}
20	12	1.239×10^{-1}	1.270×10^{-1}	1.285×10^{-1}	5.428×10^{-3}
24	12	7.958×10^{-2}	8.072×10^{-2}	8.128×10^{-2}	2.037×10^{-3}
28	12	5.363×10^{-2}	5.406×10^{-2}	5.427×10^{-2}	7.811×10^{-4}
32	12	4.149×10^{-2}	4.168×10^{-2}	4.172×10^{-2}	2.972×10^{-4}
36	12	8.572×10^{-3}	5.375×10^{-3}	5.329×10^{-3}	9.197×10^{-5}

4. CONCLUSIONS

In this study we have solved the multigroup neutron diffusion criticality problem numerically by the meshless RBF collocation method. We used the multiquadric as the RBF and worked on three problems.

We have found that, for all the problems considered, the RBF collocation yields highly accurate results for the multiplication factor and it also works well in the computation of group fluxes. It was seen that both the maximum pointwise errors in group fluxes and the error in the multiplication factor decreases with decreasing fill distance value. For the two-group problem, it was shown that, by fine-tuning of the shape parameter, the analytical result can be reproduced.

The dependence of the errors to the shape parameter has been investigated for all problems and illustrated graphically for the two-group problem. It was observed that for group fluxes the error decreases with increasing shape parameter up to a certain point. Then starts to oscillate and the numerical solution breaks down at higher values of c because of the ill-conditioning of the collocation matrix. Unlike the group fluxes, the multiplication factor has a maximum error value and it starts to increase before going into the ill-conditioned region where it does not converge to any value.

5. REFERENCES

1. G. R. Liu, *An Introduction to Meshfree Methods and Their Programming*, Springer, Netherlands, 2005.
2. E. J. Kansa, Multiquadrics-A scattered data approximation scheme with applications to computational fluid dynamics-I, *Computers and Mathematics with Applications* **19**, 127-145, 1990.
3. G. Demirkaya, C. Wafo Soh and O. J. Ilegbusi, Direct solution of Navier-Stokes equations by radial basis functions, *Applied Mathematical Modeling* **32**, 1848-1858, 2008.
4. D. L. Young, S. C. Jane, C. Y. Lin, C. L. Chiu and K. C. Chen, Solutions of 2D and 3D Stokes laws using multiquadrics method, *Engineering Analysis with Boundary Elements* **28**, 1233-1243, 2004.
5. M. Kindelan, F. Bernal, P. G. Rodriguez and M. Moscoso, Application of the RBF meshless method to the solution of the radiative transport equation, *Journal of Computational Physics* **229**, 1897-1908, 2010.
6. A. H. D. Cheng, M. A. Golberg, E. J. Kansa and G. Zammito, Exponential convergence and H-c multiquadric collocation method for partial differential equations, *Numerical Methods for Partial Differential Equations* **19**, 571-594, 2003.
7. E. Larsson and B. Fornberg, A numerical study of some radial basis function based solution methods for elliptic PDEs, *Computers and Mathematics with Applications* **46**, 891-902, 2003.
8. J. Li, A. H. D. Cheng and C. S. Chen, A comparison of efficiency and error convergence of multiquadric collocation method and finite element method, *Engineering Analysis with Boundary Elements* **27**, 251-257, 2003.
9. R. L. Hardy, Theory and Applications of the Multiquadric-Biharmonic Method 20 Years of Discovery 1968-1988, *Computers and Mathematics with Applications* **19**, 163-208, 1990
10. W. R. Madych, Miscellaneous error bounds for multiquadric and related interpolators, *Computers and Mathematics with Applications* **24**, 121-138, 1992.
11. W. M. Stacey, *Nuclear Reactor Physics*, John Wiley and Sons Inc., USA, 2001.